Environmental Science and Pollution Research (2021) 28:7191–7199
https://doi.org/10.1007/s11356-020-11058-7

RESEARCH ARTICLE

Two-dimensional transition metal phthalocyanine sheet as a promising electrocatalyst for nitric oxide reduction: a first principle study

Shiqiang Liu[1] · Yawei Liu[1] · Zhiwen Cheng[1] · Xiaoping Gao[1] · Yujia Tan[1] · Zhemin Shen[1,2,3] · Tao Yuan[1]

Received: 7 July 2020 / Accepted: 28 September 2020 / Published online: 7 October 2020

Abstract

Electrochemical reduction is a promising technology to treat polluted water contaminated by nitrate and nitrite ions under mild conditions. NO is an important intermediate species and determines selectivity toward different product and rate of whole reaction. However, the most studied NOER electrocatalysts are noble pure metal, which face problems of low utilization and high cost. Herein, by means of density functional theory computations, catalytic performance of 2D TM-Pc sheets (TM = Sc, Ti, V, Cr, Mn, Fe, Co, Ni, Cu, Zn, Nb, Mo, Ru) as NOER catalysts were systematically evaluated. Among all the studied 2D TM-Pc sheets, our results revealed 2D Co-Pc sheet was identified as the best NOER catalyst, for a proper NO absorption energy and its relatively low limiting potential. The final reduction product of NOER is either NH_3 at low coverages with energy input of 0.58 eV or N_2O at high coverages with no energy barrier. Moreover, 2D Co-Pc sheet can efficiently suppress the competing HER. This study could not only provide a new approach for electrochemical denitrification to resolve environmental pollution but also be useful for valuable ammonia production.

Keywords NO electroreduction reaction · Polluted water treatment · SACs · Ammonia · 2D TM-pc sheet · First principle

Introduction

Nitrogen is one of the most abundant and important elements in the human body, which can be converted to a wide range of inorganic compounds, including nitrate (NO_3^-), nitrite (NO_2^-), nitric oxide (NO), nitrous oxide (N_2O), ammonia (NH_3), and so on (Canfield et al. 2010a; Galloway et al. 2008). Through the biological action of nitrifying bacteria and denitrifying bacteria, NH_3 is converted to NO_2^- and NO_3^-, and then it goes back to N_2, completing the cycle of nitrogen in nature (Anonymous 2011; Miller et al. 2006). Although NO_2^- and NO_3^- are naturally present at low concentrations, artificial sources lead to elevated NO_2^- and NO_3^- levels, such as overfertilization in agriculture and large-scale animal husbandry (Seiler 2005). Because of low efficiency of nitrogenous fertilizer, about 20% of the nitrogenous fertilizer globally is lost through leaching (Clark et al. 2020). Continuous accumulations of NO_2^- and NO_3^- ions in surface and ground water lead to water pollution. Ingestion of NO_2^- and NO_3^- ions in high concentrations can lead severe healthy problem, causing methemoglobinemia, liver damage, and cancer (Duca and Koper 2012). NO_2^- is the primary reduction product of NO_3^-, and NO_2^- can react with amines and amides, generating potentially carcinogenic N-nitrosamine compound byproducts (Nolan et al. 2000). Therefore, strict regulations on maximum concentrations of NO_2^- and NO_3^- in drinking water have been issued by the World Health Organization, which are 0.5 mg/L and 50 mg/L, respectively (Duca and Koper 2012). As a result, reducing concentrations of NO_2^-

Responsible editor: Weiming Zhang

Electronic supplementary material The online version of this article (https://doi.org/10.1007/s11356-020-11058-7) contains supplementary material, which is available to authorized users.

✉ Tao Yuan
taoyuan@sjtu.edu.cn

[1] School of Environmental Science and Engineering, Shanghai Jiao Tong University, Shanghai 200240, People's Republic of China

[2] Shanghai Engineering Research Center of Solid Waste Treatment and Resource Recovery, Shanghai 200240, People's Republic of China

[3] Shanghai Institute of Pollution Control and Ecological Security, Shanghai 200092, People's Republic of China

and NO_3^- on an industrial scale, two of the most widely found contaminants in drinking water, have become an important environmental concern.

Compared with conventional water treatment methods, electrochemical denitrification has been proven to be an effective and alternative technology to water denitrification (Della Rocca et al. 2007; Fan et al. 2009; Fanning 2000; Huang et al. 1998). During NO_3^- and NO_2^- electroreduction, complicated reaction product and byproduct can be generated, such as NO, N_2O, N_2, NH_3OH^+, and NH_4^+ (de Groot and Koper 2004; Figueiredo et al. 2013; Molodkina et al. 2012). Among the various products and byproducts, NO is considered to be the key intermediate species and determines selectivity toward different products and rates of the whole reaction. Therefore, there is a considerable interest and great importance to understand the nature of NO's transformations (Duca and Koper 2012; Rosca et al. 2009). However, developing new novel and effective NO electroreduction reaction (NOER) catalysts presents a major unsolved but highly payback challenge.

Additional, fewer previous studies focus on selectivity toward ammonia (NH_3), for its toxicity on human health and pollution in the air (Yin et al. 2018). Ammonia, a crucial precursor to nitrogenous fertilizer to sustain the global food supply, is considered as one of most important chemical feedstock (Canfield et al. 2010b; Erisman et al. 2008; Galloway et al. 2008). NH_3 also has a great potential to apply in fuel cell technologies, for its high energy density (Afif et al. 2016; Fuerte et al. 2009). It is of great significant to produce this valuable byproduct in the electrochemical denitrification process. Considering the combination of water treatment and valuable NH_3 production, we are motivated to discover new NOER catalysts that favor NH_3 over N_2 formation to treat water contaminated by NO_2^- and NO_3^- ions.

In recent years, studies on NOER catalysts mainly focus on pure transition metals catalyst, such as Pt, Cu, and Au (Chun et al. 2017; Farberow et al. 2014). However, low utilization and high cost of pure noble metal catalyst required for this process hamper applications on an industrial scale and inspire continued efforts to identify alternatives catalysts. Single-atom catalysts (SACs), decorating catalytically active and isolated metal atoms on the substrate, emerged in recent years and offer us an effective way to solve the metal utilization and cost problems (Azofra et al. 2017; Jin et al. 2018; Qiao et al. 2011; Qiu et al. 2015; Yang et al. 2013). Thus, SACs have already been considered as promising candidates for versatile catalytic reactions, such as the CO oxidation reaction, CO_2 reduction reaction, hydrogen evolution reaction, oxygen reduction reaction, oxygen evolution reaction, N_2 reduction reaction, and propane dehydrogenation (He et al. 2018; Li et al. 2019; Li et al. 2016; Ling et al. 2017; Liu et al. 2019; Lv et al. 2019; Ma et al. 2015; Ma et al. 2016; Ma et al. 2019; Niu et al. 2019; Patel et al. 2018; Shen et al. 2015; Varela et al. 2019; Wang et al. 2019b; Wang et al. 2015; Zhang et al. 2018).

Organometallic porous sheets, providing intrinsic evenly distributed binding sites which can firmly anchor single TM atoms and prevent TM atoms aggregation into cluster, have recently attracted considerable attention.(Li and Sun 2014; Liu et al. 2019; Liu et al. 2020; Sun et al. 2015) Among several kinds of organometallic porous sheets, phthalocyanine (Pc) provides abundant binding sites, a plane consisting of four isoindole rings, for TM atom (Zhu et al. 2014). Therefore, Pc is an ideal substrate and attracts many researchers to explore its catalytic performance on various catalytic reactions (Deng et al. 2013; Jia et al. 2018; Li and Sun 2014; Liu et al. 2020). Besides, phthalocyanine can be synthesized massively in low cost. This advantage makes 2D TM-Pc sheet catalysts suitable for large-scale industrial application (Dahlen 1939; Li et al. 2008; Yuen et al. 2012). Inspired by the excellent catalytic activity of 2D TM-Pc sheets, a theoretical study on this issue will shed some light on developing and facilitating NOER catalysts.

To achieve this aim, the catalytic activity of 2D TM-Pc sheets (TM = Sc, Ti, V, Cr, Mn, Fe, Co, Ni, Cu, Zn, Nb, Mo, Ru) toward NOER have been screened with first-principles calculations in this work. On the basis of our comprehensive computational work, 2D Co-Pc sheet was identified to be the best NOER catalyst among all candidates due to small energy input of the whole process. The Gibbs free energy for each elementary reaction was derived to find which pathway is more favorable in Gibbs free energy for NOER. NH_3 is the main product at low coverages through the HNO* intermediate species, while N_2O can be easily formed at high coverages.

Computational methods

In this work, all optimizations and vibrational frequency calculations of these structures were performed by using spin-polarized density-functional theory methods implemented in Vienna ab initio Simulation Package (Kresse and Furthmüller 1996; Kresse and Hafner 1993). The generalized gradient approximation (GGA) functional in the form proposed by Perdew-Burke-Ernzerhof (PBE) was employed to describe the electron exchange correlation interactions (Perdew et al. 1992; Perdew and Wang 1992). The electron-ion interactions were described by projector augmented wave potentials (Blöchl 1994). Energy cutoff and convergence criteria for the residual force and energy were set to be 500 eV, 0.01 eV/Å, and 1×10^{-5} eV, respectively. The first Brillouin zone was sampled with a $5 \times 5 \times 1$ k-points using the Monkhorst−Pack mesh scheme (Monkhorst and Pack 1976). All of the 2D TM-Pc sheets were modeled with periodic monolayer of primitive cell, which is consisted of 20 C atoms, 8 N atoms, 4 H atoms, and 1 TM atom. The dispersion correction has been considered using the DFT-D_3 method with

the standard parameters programmed by Grimme and co-workers (Grimme et al. 2010). A vacuum space of 20 Å in the *z*-direction was set, which is enough to avoid interactions between two neighbor TM-Pc images, during the structure relaxation. For electronic structure calculations, a denser 9 × 9 × 1 k-points grid was applied. In addition, the NOER performance was evaluated by the reaction Gibbs free energy change (ΔG). We computed the Gibbs free energy change (ΔG) of every elemental step using computational hydrogen electrode (CHE) model proposed by Nørskov et al. (Nørskov et al. 2004). Further details regarding electrochemical reactions and selectivity *f* of NOER toward different reactions are given in the Supporting Information.

Results and discussion

Geometric structures of the 2D TM-Pc sheet

The geometric properties of the 2D TM-Pc sheets were first studied. Structurally, we found that the optimized 2D Pc sheet can still remain flat without any bulking after embedding these TM atoms. Optimized geometric structure of 2D TM-Pc sheet is shown in Fig. 1 and primitive unit cell is marked by a gray line. The optimized lattice parameter of 2D Fe-Pc sheet agrees with experimental value and theoretical value very well (Abel et al. 2011; Wang et al. 2015; Zhou and Sun 2011). The optimized lattice parameters of 2D Co, Cr-Pc sheet are also in good agreement with other theoretical studies (Deng et al. 2013; Li and Sun 2014).

Screening 2D TM-Pc sheets as NOER Electrocatalyst

The adsorption of NO on catalyst surface is a prerequisite to initialize the NOER. According to previous theoretical studies, initial configuration of NO adsorption on 2D TM-Pc sheet is vital in the subsequent reaction pathway. Herein, we first tested both end-on and side-on configurations to investigate the interaction strength of NO molecule adsorption on 2D TM-Pc sheet. In end-on configurations, both the atoms of the NO molecule attached to the central TM atom were considered.

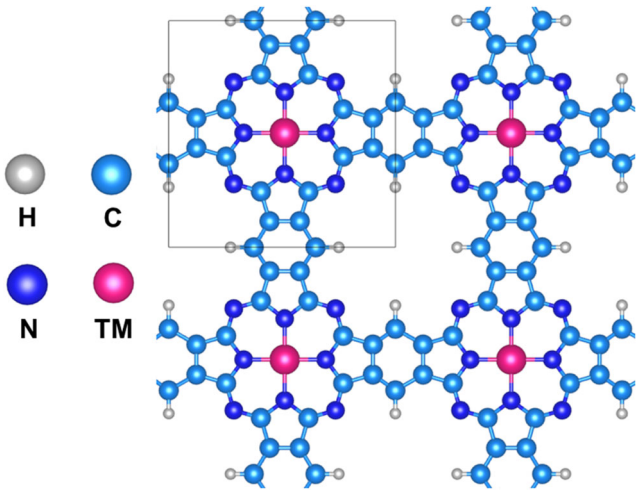

Fig. 1 The optimized geometric structures of 2D TM-Pc sheet in 2 × 2 supercell cell. The primitive unit cell is marked by a gray line

According to the classical Sabatier principle in catalysis, the Gibbs free energy of NO absorption on an ideal NOER catalyst is expected to be moderate (Nørskov et al. 2005). The chemisorption adsorption will sufficiently activate NO molecule to participate in the following redox reaction. However, too strong chemical adsorption will result in difficulties for the product to dissociate from the catalyst surface. Therefore, interactions between NO and an ideal catalyst should be as weak as possible, but strong enough to prevent desorption.

To find the right catalyst to initialize the NOER, we screened a series of transition metal atoms, including Sc, Ti, V, Cr, Mn, Fe, Co, Ni, Cu, Zn, Nb, Mo, and Ru, anchored on 2D Pc sheets. The ΔG of absorption results show that NO is more inclined to bind with the central TM atom in end-on configuration via N atom, forming TM–N bonds (Fig. 2a). The bond lengths of N–O and interaction strength of NO molecule adsorption on 2D TM-Pc sheets are shown in Fig. 3. After the NO absorption on the 2D TM-Pc sheets, N–O bond length is stretched to varying degrees, compared with that of the isolated NO molecule. According to above criterion, 2D Ni, Cu, Zn-Pc sheets are not appropriate as NOER electrocatalysts for positive adsorption Gibbs free energies. Hence, 2D Co-Pc sheet is expected to be the best candidate NOER catalyst, among all above studied 2D TM-Pc sheets, while the other 2D TM-Pc sheets exhibit too strong interaction with NO. Meanwhile, the N–O bond length is elongated from 1.172 Å in a free NO gas molecule to 1.181 Å after the absorption on 2D Co-Pc sheet, suggesting effective activation of the NO molecule. Thus, in the subsequent parts, the whole process of NOER on the 2D Co-Pc sheet will be further explored.

NO adsorption on 2D Co-Pc sheet with different coverages

According to previous reports, coverages of NO are principal factors to influence the product of NOER (de Vooys et al. 2001a, b; Wang et al. 2018). After screening out 2D Co-Pc sheet as a potential NOER catalyst candidate, we further investigated interactions between NO molecule and 2D Co-Pc sheet at different coverages.

At low coverages, three initial configurations of NO adsorption on 2D Co-Pc sheet were considered, as shown in Fig. 2. After a full structure relaxation, side-on configuration spontaneously transforms into the end-on configuration, and the NO molecule is binding to the central Co atom via N atom.

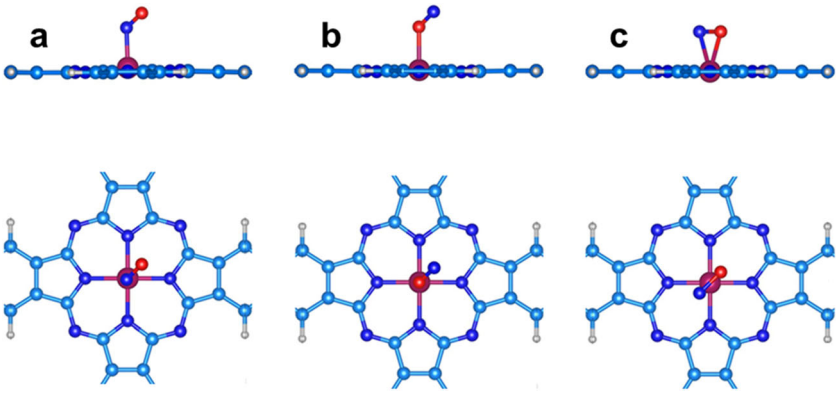

Fig. 2 Top and side views of 2D TM-Pc sheets with (a), (b) end-on and (c) side-on NO adsorption configurations

For the end-on configurations, N atom of NO molecule intends to be attached with the central Co atom with a Co–N bond length of 1.816 Å, which has more negative absorption energy. To explore the intrinsic mechanisms of NO adsorption on 2D Co-Pc sheet, charge density difference and the partial densities of states (PDOS) were used to illuminate the interaction between NO molecule and 2D Co-Pc sheet.

As shown in Fig. 4, there is an obvious hybridization between the N-2p orbitals and the Co-3d orbitals. It can be found that when the NO molecule is adsorbed on the central Co atom, charge accumulation and depletion can be observed for both the NO molecule and Co atom. The Bader charge analysis confirms the speculate that about 0.07 electrons transfer from 2D Co-Pc sheet to NO molecule, meaning that electrons transfer from the Co-3d orbital to the empty N-2π* orbital, leading to a partially occupied 2π* orbital. Charge density is accumulated around the NO molecule, improving the activity of NO, which helps facilitate the subsequent hydrogenation reaction (Fig. 5).

At high coverages, we investigated NO adsorption on 2D Co-Pc sheet as $(NO)_2$ dimer, because the dimer could be reduced, forming N_2O (Wang et al. 2018). After examining several different initial configurations (Fig. S1), the energetically favorable configuration was obtained and shown in Fig. 6.

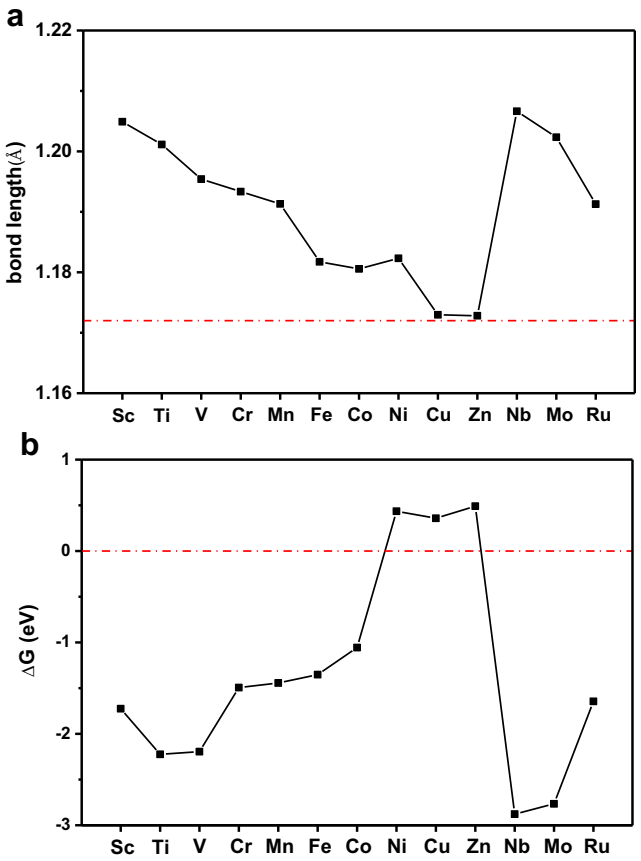

Fig. 3 (a) N–O bond length (Å) and (b) adsorption free energy (ΔG) for NO adsorbed on 2D TM-Pc sheets. The red dashed line represents N–O bond length of free NO gas molecule and ΔG = 0 eV, respectively

Catalytic performance on NOER

After confirming the energetically favorable configuration of NO adsorption on 2D Co-Pc sheet, we further investigated the following NOER steps on 2D Co-Pc sheet and selectivity of different pathways (Fig. 7).

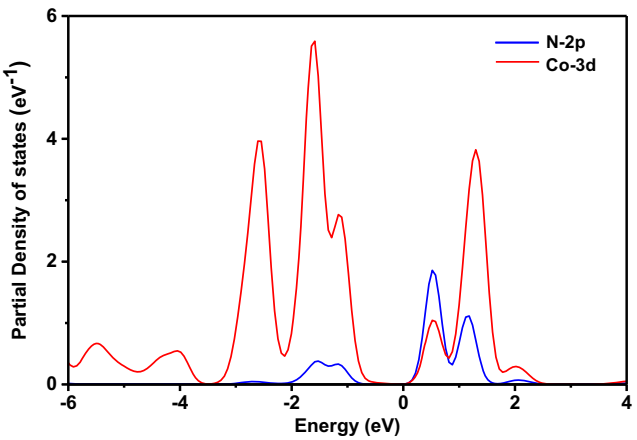

Fig. 4 The computed PDOS of NO adsorbed on the 2D Co-Pc sheet in end-on configuration

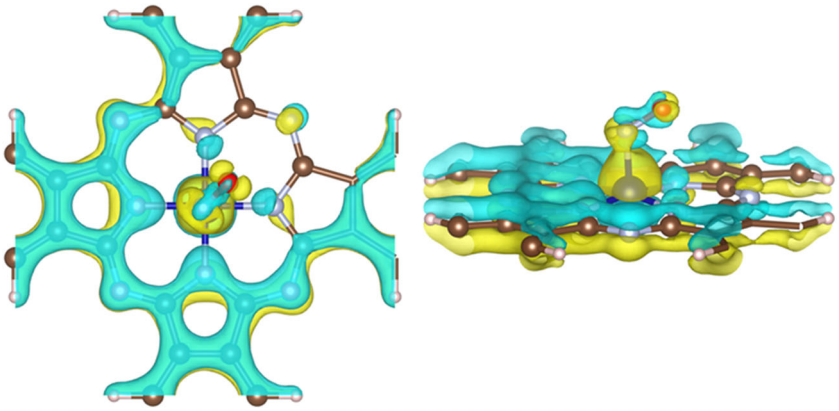

Fig. 5 Charge density difference of NO adsorbed on the 2D Co-Pc sheet in end-on configuration. The positive and negative charges are shown in yellow and cyan

NH_3 formation at low coverages

The adsorbed NO starts to hydrogenate by interacting with proton coupled with electron. As first hydrogenation reaction is possible to occur at either atom of the adsorbed NO, different intermediates species can be formed and NOER on 2D Co-Pc sheet will follow different pathways. Providing the adsorbed NO will be hydrogenated by adsorbing a proton coupled with an electron in the distal O site, forming an NOH* intermediate species adsorbed on the 2D Co-Pc sheet, an energy input of 1.28 eV is required and the N-O bond length is further elongated to 1.343 Å. In the following step, NOH* will be further hydrogenated through two possible reaction pathways: (1) The distal O atom is spontaneously hydrogenated, releasing a H_2O molecule and forming N* intermediate species, with an energy output of 0.06 eV. (2) N atom is the second hydrogenation site, forming HNOH* intermediate species. The free energy goes downhill for 0.52 eV. Different hydrogenation sites compete in the second hydrogenation reaction. The selectivity *f* toward formation of HNOH* is almost 1. Therefore, the HNOH* could be the favored intermediates and the NOER prefers to proceed through the second pathway after the formation of NOH* intermediate species. Then, the hydrogenation reaction occurs at the distal O, releasing the H_2O molecule and forming NH* species. Then, NH* intermediate species is continuously hydrogenated until formation of the NH_3. The ΔG values for the three steps are − 0.05, − 2.09, and 1.35 eV, respectively. The ΔG for NH_3 desorption form 2D Co-Pc sheet surface is 0.23 eV. Formation of NOH* intermediate species is the rate-limiting step with maximum energy consumption ΔG = 1.28 eV during the whole process.

When the N atom of NO molecules will be first hydrogenated, HNO* intermediate species can be formed, with an N–O bond length of 1.243 Å. The free energy goes uphill for 0.58 eV. In the second hydrogenation, both atoms of the adsorbed NO are possible hydrogenation sites. When the distal O atom is hydrogenated, this step needs to overcome a Gibbs free energy barrier of 0.19 eV, while the N atom is spontaneously hydrogenated and ΔG of this step is downhill by 0.14 eV. This step is exothermal reaction, which means that HNO* can spontaneously adsorb a proton coupled with an electron in N atom. The selectivity *f* toward formation of H_2NO* is almost 1, which implies the second hydrogenation reaction prefers to occur in the N atom. In the following steps, H_2NO* intermediate species will be sequentially hydrogenated in distal O atom until a H_2O molecule is released. Then, NH_2* intermediate species will be further hydrogenated and NH_3* can be formed. ΔG for the three steps are − 0.75, − 1.05, and − 1.35 eV, respectively. The first hydrogenation

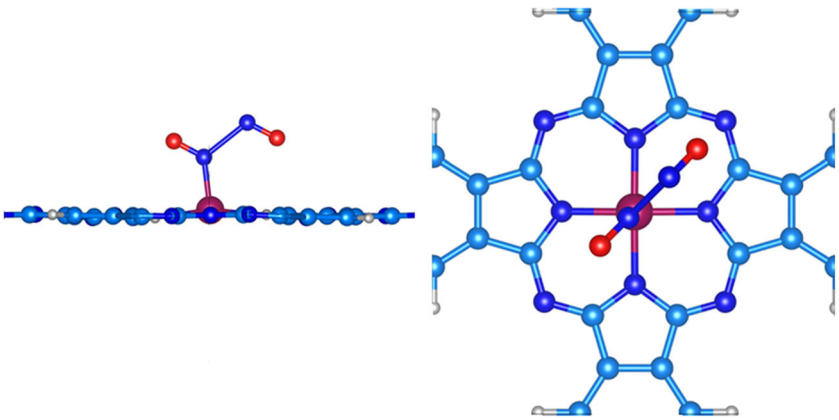

Fig. 6 Top and side views of NO adsorption on 2D Co-Pc sheet as $(NO)_2$ dimer

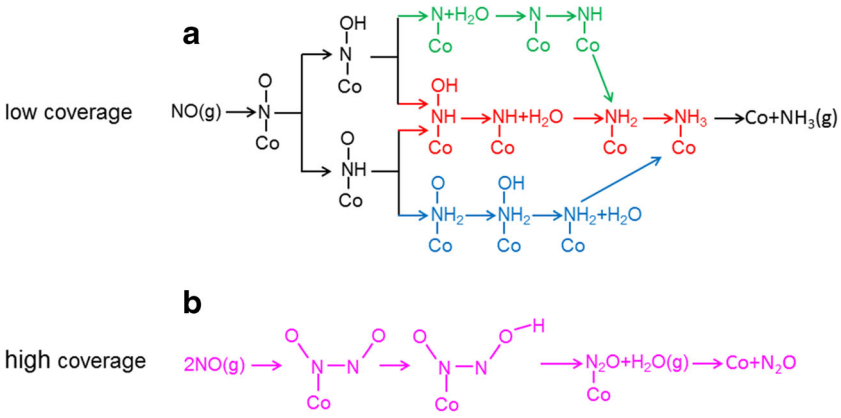

Fig. 7 Schematic depiction of the pathways of NO electrochemical reduction on the 2D Co-Pc sheet at (a) low and (b) high coverages

reaction is the rate-limiting step with maximum energy consumption $\Delta G = 0.58$ eV during the whole process (Fig. 8).

Therefore, the last pathway is energetically favorable among the four possible reaction pathways, for small energy requirements of the former two hydrogenation reaction.

N_2O formation at high coverages

In addition to ammonia, N_2O could be one of the products during the NO electroreduction reaction at high coverages. The results show Gibbs free energy of $(NO)_2$ dimer absorption on 2D Co-Pc sheet is downhill by 0.71 eV, and the energetically favorable configuration is the *trans*-$(NO)_2$* intermediate species. The *trans*-$(NO)_2$* can be spontaneously hydrogenated by adsorbing a proton coupled with an electron, forming an HONNO* intermediate species. Gibbs free energy of this step decreases by 0.08 eV. Then, the newly formed HONNO* species spontaneously absorbs another a proton coupled with an electron and release a H_2O molecule, forming N_2O* intermediate species. Our calculations show that it is difficult for N_2O to absorb on 2D Co-Pc sheet, for a positive absorption free energy of 0.31 eV. Overall, at high coverages, NO can be effectively absorbed on 2D Co-Pc sheet as $(NO)_2$ dimer. Then, the intermediate species can be hydrogenated and product N_2O can detach spontaneously, and no energy barrier is involved (Fig. 9).

Herein, the NOER on 2D Co-Pc sheet may kinetically prefer the N_2O formation rather than the NH_3 formation. However, although this pathway is possible at high NO surface coverages, NO prefers to be absorbed on 2D Co-Pc sheet other than absorbing neighboring NO molecules, due to the very strong N–Co interaction and relatively weak N–N bond. Besides, the actual NO concentration could not be too high, so an applied potential is necessary to trigger NO reduction.

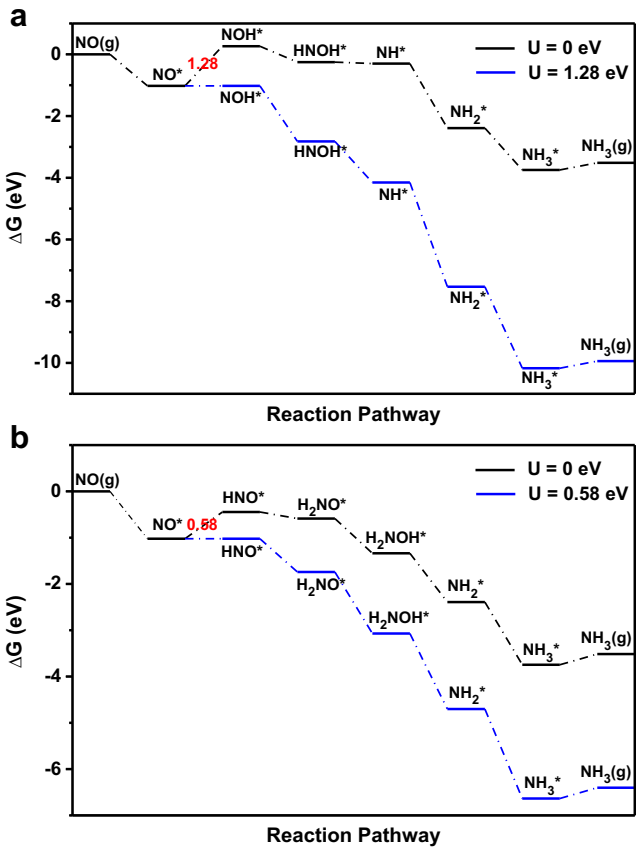

Fig. 8 The Gibbs free energy profiles of the NORR on 2D Co-Pc sheet along the second pathway and the fourth pathway

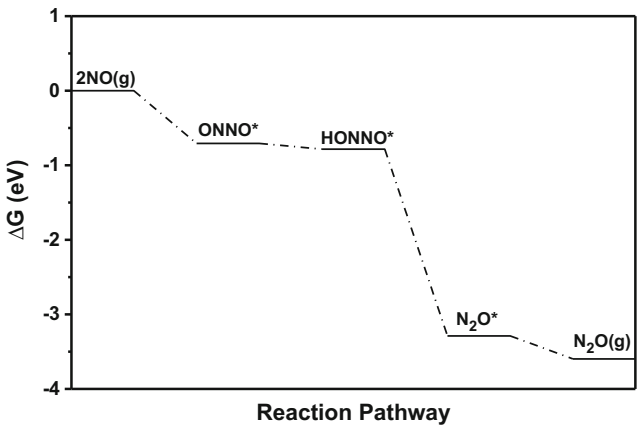

Fig. 9 The Gibbs free energy profiles of the NORR on 2D Co-Pc sheet at high coverage

Charge population along the pathways

To further investigate the microscopic scenario behind catalytic performance of the 2D Co-Pc sheet, the charge variation of each reaction step is analyzed, shown in Fig. S2. Each intermediate species along with the pathway was divided into three parts: Pc substrate, central metal atom Co, and adsorbate intermediates spices. As shown in Fig. S2, at low coverages, obvious electron transfer occurs for the three parts along the fourth pathway. Initially, the end-on adsorbed NO gains 0.07 electrons, which is attributed to donation by central metal atom Co. After the first hydrogenation, NHO* intermediates spices gains another 0.07 electrons from 2D Co-Pc sheet. For the following steps, the adsorbate intermediate species gain 0.06, − 0.10, 0.15 0.32, and − 0.33 electrons respectively, while Pc substrates lose 0.01, − 0.09, − 0.16, 0.27, and − 0.29 electrons respectively. At high coverages, at the first step, $(NO)_2$ adsorption, about 0.17 electrons transferred from 2D Co-Pc sheet to ONNO* intermediates spices. For the following steps, the adsorbate intermediate species gain 0.14, and − 0.30 electrons respectively, while Pc substrates lose 0.07 and − 0.40 electrons respectively. As the hydrogenation proceeds, charge population of the central metal atom Co is relatively stable. Hence, central metal atom Co acts as a transmitter, transferring electrons between Pc substrate and the adsorbate spices.

Competition with the HER

Considering that the hydrogen evolution reaction (HER) is highly likely to occur in the presence of water, suppressing HER is the major concern for the NOER catalyst. We calculated the adsorption ΔG for H on 2D Co-Pc sheet, and the value is positive (0.21 eV), indicating it is difficult for central Co atom to adsorb H atoms. The interaction of H atom on Co atom is much weaker than that of NO, implying that the adsorption of NO is preferred and the adsorption of hydrogen is energetically unfavorable. The 2D Co-Pc sheet is demonstrated to be more selective for the NOER than for the HER in aqueous solution. Strong interaction between H_2O molecule and available active sites of the catalyst can severely hamper NOER efficiency. Competitive adsorption of H_2O and NO on 2D Co-Pc sheet was also taken into consideration. The value of adsorption ΔG of H_2O on 2D Co-Pc is 0.04 eV, indicating that the H_2O molecule could not be stably adsorbed.

Recently, 2D Co-Pc sheet has been synthesized successfully in experiments and the stability of 2D Co-Pc sheet is well guaranteed (Epstein and Wildi 1960; Huang et al. 2020; Liu et al. 2020; Liu and McCrory 2019; Wang et al. 2019a; Wang et al. 2015). The 2D Co-Pc sheet also exhibits good electrical conductivity for a fully π-conjugated network and stability for strong coordination bond of TM-Pc. Since 2D Co-Pc sheet achieves the combination of conductivity, stability, and catalytic activity, the unique features significantly actualize the utilization of the 2D Co-Pc sheet catalyst on the NOER.

Conclusions

In summary, by means of DFT calculations, we systematically explored the potential application of 2D TM-Pc (TM = Sc, Ti, V, Cr, Mn, Fe, Co, Ni, Cu, Zn, Nb, Mo, Ru) sheets as NO reduction electrocatalysts at mild conditions. According to our screening criteria, among all studied 2D TM-Pc sheets, 2D Co-Pc sheet is considered as the most promising electrocatalysts, which has a moderate absorption Gibbs free energy. NH_3 can be formed through the HNO* intermediate species at low coverages with an energy input of 0.58 eV, while at high coverages, N_2O can be easily formed with no energy barrier. More importantly, the competing HER can be well suppressed. Therefore, we propose 2D Co-Pc sheet as a promising electrocatalyst for NOER at mild conditions. We hope this work could provide useful guidance to further explore more electrochemical denitrification methods that combine polluted water treatment and worthy byproduct production, in both experiment and theory.

Authors' contributions All authors discussed the results and assisted during manuscript preparation. Shiqiang Liu performed the research, analyzed result, and wrote the manuscript. Yawei Liu helped in designing the research and analyzing the result. Zhiwen Cheng regulated the research and anticipated discussion. Xiaoping Gao edited the manuscript. Yujia Tan edited the manuscript. Tao Yuan provided ideas and supervised the research. Zhemin Shen supplied software copyright.

Funding This work is supported by the National Water Pollution Control Key Project: 2017ZX07202005-005, and the Medicine & Engineering Collaborative Research Fund of Shanghai Jiao Tong University (No.YG2019ZDA29).

Data availability Not applicable

Compliance with ethical standards

Competing interests The authors declare that they have no competing interests.

Ethical approval Not applicable

Consent to participate Not applicable

Consent to publish Not applicable

References

Abel M, Clair S, Ourdjini O, Mossoyan M, Porte L (2011) Single layer of polymeric Fe-phthalocyanine: an organometallic sheet on metal and thin insulating film. J Am Chem Soc 133:1203–1205

Afif A, Radenahmad N, Cheok Q, Shams S, Kim JH, Azad AK (2016) Ammonia-fed fuel cells: a comprehensive review. Renew Sust Energ Rev 60:822–835

Anonymous (2011) The European nitrogen assessment: sources, effects and policy perspectives. Cambridge University Press, Cambridge

Azofra LM, Sun C, Cavallo L, MacFarlane DR (2017) Feasibility of N2 binding and reduction to ammonia on Fe-deposited MoS2 2D sheets: a DFT study. Chem Eur J 23:8275–8279

Blöchl PE (1994) Projector augmented-wave method. Phys Rev B 50: 17953–17979

Canfield DE, Glazer AN, Falkowski PG (2010a) The evolution and future of Earth's nitrogen cycle. Science 330:192–196

Canfield DE, Glazer AN, Falkowski PG (2010b) The evolution and future of Earth's nitrogen cycle. Science 330:192–196

Chun H-J, Apaja V, Clayborne A, Honkala K, Greeley J (2017) Atomistic insights into nitrogen-cycle electrochemistry: a combined DFT and kinetic Monte Carlo analysis of NO electrochemical reduction on Pt(100). ACS Catal 7:3869–3882

Clark CA, Reddy CP, Xu H, Heck KN, Luo G, Senftle TP, Wong MS (2020) Mechanistic insights into pH-controlled nitrite reduction to ammonia and hydrazine over rhodium. ACS Catal 10:494–509

Dahlen MA (1939) The phthalocyanines a new class of synthetic pigments and dyes. Ind Eng Chem 31:839–847

de Groot MT, Koper MTM (2004) The influence of nitrate concentration and acidity on the electrocatalytic reduction of nitrate on platinum. J Electroanal Chem 562:81–94

de Vooys ACA, Koper MTM, van Santen RA, van Veen JAR (2001a) Mechanistic study of the nitric oxide reduction on a polycrystalline platinum electrode. Electrochim Acta 46:923–930

de Vooys ACA, Koper MTM, van Santen RA, van Veen JAR (2001b) Mechanistic study on the Electrocatalytic reduction of nitric oxide on transition-metal electrodes. J Catal 202:387–394

Della Rocca C, Belgiorno V, Meriç S (2007) Overview of in-situ applicable nitrate removal processes. Desalination 204:46–62

Deng Q, Zhao L, Gao X, Zhang M, Luo Y, Zhao Y (2013) Single layer of polymeric cobalt phthalocyanine: promising low-cost and high-activity nanocatalysts for CO oxidation. Small 9:3506–3513

Duca M, Koper MTM (2012) Powering denitrification: the perspectives of electrocatalytic nitrate reduction. Energy Environ Sci 5:9726–9742

Epstein A, Wildi BS (1960) Electrical properties of poly-copper phthalocyanine. J Chem Phys 32:324–329

Erisman JW, Sutton MA, Galloway J, Klimont Z, Winiwarter W (2008) How a century of ammonia synthesis changed the world. Nat Geosci 1:636–639

Fan X, Guan X, Ma J, Ai H (2009) Kinetics and corrosion products of aqueous nitrate reduction by iron powder without reaction conditions control. J Environ Sci 21:1028–1035

Fanning JC (2000) The chemical reduction of nitrate in aqueous solution. Coord Chem Rev 199:159–179

Farberow CA, Dumesic JA, Mavrikakis M (2014) Density functional theory calculations and analysis of reaction pathways for reduction of nitric oxide by hydrogen on Pt(111). ACS Catal 4:3307–3319

Figueiredo MC, Solla-Gullón J, Vidal-Iglesias FJ, Climent V, Feliu JM (2013) Nitrate reduction at Pt(100) single crystals and preferentially oriented nanoparticles in neutral media. Catal Today 202:2–11

Fuerte A, Valenzuela RX, Escudero MJ, Daza L (2009) Ammonia as efficient fuel for SOFC. J Power Sources 192:170–174

Galloway JN, Townsend AR, Erisman JW, Bekunda M, Cai Z, Freney JR, Martinelli LA, Seitzinger SP, Sutton MA (2008) Transformation of the nitrogen cycle: recent trends, questions, and potential solutions. Science 320:889–892

Grimme S, Antony J, Ehrlich S, Krieg H (2010) A consistent and accurate ab initio parametrization of density functional dispersion correction (DFT-D) for the 94 elements H-Pu. J Chem Phys 132:154104

He B, Shen J, Ma D, Lu Z, Yang Z (2018) Boron-doped C3N monolayer as a promising metal-free oxygen reduction reaction catalyst: a theoretical insight. J Phys Chem C 122:20312–20322

Huang C-P, Wang H-W, Chiu P-C (1998) Nitrate reduction by metallic iron. Water Res 32:2257–2264

Huang N, Lee KH, Yue Y, Xu X, Irle S, Jiang Q, Jiang D (2020) A Stable and conductive metallophthalocyanine framework for electrocatalytic carbon dioxide reduction in water. Angew Chem Int Ed 59: 16587–16593

Jia H, Yao Y, Zhao J, Gao Y, Luo Z, Du P (2018) A novel two-dimensional nickel phthalocyanine-based metal–organic framework for highly efficient water oxidation catalysis. J Mater Chem A 6: 1188–1195

Jin H, Guo C, Liu X, Liu J, Vasileff A, Jiao Y, Zheng Y, Qiao S-Z (2018) Emerging two-dimensional nanomaterials for electrocatalysis. Chem Rev 118:6337–6408

Kresse G, Hafner J (1993) Ab initio molecular dynamics for open-shell transition metals. Phys Rev B 48:13115–13118

Kresse G, Furthmüller J (1996) Efficiency of ab-initio total energy calculations for metals and semiconductors using a plane-wave basis set. Comput Mater Sci 6:15–50

Li L, Tang Q, Li H, Hu W, Yang X, Shuai Z, Liu Y, Zhu D (2008) Organic thin-film transistors of phthalocyanines, Pure and Applied Chemistry, pp 2231

Li Q, Qiu S, Liu C, Liu M, He L, Zhang X, Sun C (2019) Computational design of single-molybdenum catalysts for the nitrogen reduction reaction. J Phys Chem C 123:2347–2352

Li X-F, Li Q-K, Cheng J, Liu L, Yan Q, Wu Y, Zhang X-H, Wang Z-Y, Qiu Q, Luo Y (2016) Conversion of dinitrogen to ammonia by FeN3-embedded graphene. J Am Chem Soc 138:8706–8709

Li Y, Sun Q (2014) The superior catalytic CO oxidation capacity of a Cr-phthalocyanine porous sheet. Sci Rep 4:4098

Ling C, Shi L, Ouyang Y, Zeng XC, Wang J (2017) Nanosheet supported single-metal atom bifunctional catalyst for overall water splitting. Nano Lett 17:5133–5139

Liu J-H, Yang L-M, Ganz E (2019) Electrocatalytic reduction of CO2 by two-dimensional transition metal porphyrin sheets. J Mater Chem A 7:11944–11952

Liu S, Liu Y, Gao X, Tan Y, Shen Z, Fan M (2020) First principle study of feasibility of dinitrogen reduction to ammonia on two-dimensional transition metal phthalocyanine monolayer. Appl Surf Sci 500:144032

Liu Y, McCrory CCL (2019) Modulating the mechanism of electrocatalytic CO2 reduction by cobalt phthalocyanine through polymer coordination and encapsulation. Nat Commun 10:1683

Lv X, Wei W, Zhao P, Er D, Huang B, Dai Y, Jacob T (2019) Oxygen-terminated BiXenes and derived single atom catalysts for the hydrogen evolution reaction. J Catal 378:97–103

Ma DW, Li T, Wang Q, Yang G, He C, Ma B, Lu Z (2015) Graphyne as a promising substrate for the noble-metal single-atom catalysts. Carbon 95:756–765

Ma DW, Wang Q, Yan X, Zhang X, He C, Zhou D, Tang Y, Lu Z, Yang Z (2016) 3d transition metal embedded C2N monolayers as promising single-atom catalysts: a first-principles study. Carbon 105: 463–473

Ma X, Hu J, Zheng M, Li D, Lv H, He H, Huang C (2019) N2 reduction using single transition-metal atom supported on defective WS2 monolayer as promising catalysts: a DFT study. Appl Surf Sci 489:684–692

Miller SA, Landis AE, Theis TL (2006) Use of Monte Carlo analysis to characterize nitrogen fluxes in agroecosystems. Environ Sci Technol 40:2324–2332

Molodkina EB, Botryakova IG, Danilov AI, Souza-Garcia J, Feliu JM (2012) Mechanism of nitrate electroreduction on Pt(100). Russ J Electrochem 48:302–315

Monkhorst HJ, Pack JD (1976) Special points for Brillouin-zone integrations. Phys Rev B 13:5188–5192

Nørskov JK, Rossmeisl J, Logadottir A, Lindqvist L, Kitchin JR, Bligaard T, Jónsson H (2004) Origin of the overpotential for oxygen reduction at a fuel-cell cathode. J Phys Chem B 108:17886–17892

Nørskov JK, Bligaard T, Logadottir A, Kitchin JR, Chen JG, Pandelov S, Stimming U (2005) Trends in the exchange current for hydrogen evolution. J Electrochem Soc 152:J23

Niu K, Qi Z, Li Y, Lin H, Chi L (2019) Theoretical investigation of on-purpose propane dehydrogenation over the two-dimensional Ru–Pc framework. J Phys Chem C 123:4969–4976

Nolan B, Stoner T, Jeffrey D (2000) Nutrients in groundwaters of the conterminous United States, 1992-1995. Environ Sci Technol

Patel AM, Ringe S, Siahrostami S, Bajdich M, Nørskov JK, Kulkarni AR (2018) Theoretical approaches to describing the oxygen reduction reaction activity of single-atom catalysts. J Phys Chem C 122: 29307–29318

Perdew JP, Chevary JA, Vosko SH, Jackson KA, Pederson MR, Singh DJ, Fiolhais C (1992) Atoms, molecules, solids, and surfaces: applications of the generalized gradient approximation for exchange and correlation. Phys Rev B 46:6671–6687

Perdew JP, Wang Y (1992) Accurate and simple analytic representation of the electron-gas correlation energy. Phys Rev B 45:13244–13249

Qiao B, Wang A, Yang X, Allard LF, Jiang Z, Cui Y, Liu J, Li J, Zhang T (2011) Single-atom catalysis of CO oxidation using Pt1/FeOx. Nat Chem 3:634–641

Qiu H-J, Ito Y, Cong W, Tan Y, Liu P, Hirata A, Fujita T, Tang Z, Chen M (2015) Nanoporous graphene with single-atom nickel dopants: an efficient and stable catalyst for electrochemical hydrogen production. Angew Chem Int Ed 54:14031–14035

Rosca V, Duca M, de Groot MT, Koper MTM (2009) Nitrogen cycle electrocatalysis. Chem Rev 109:2209–2244

Seiler RL (2005) Combined use of N-15 and O-18 of nitrate and B-11 to evaluate nitrate contamination in groundwater. Appl Geochem 20: 1626–1636

Shen J, Kortlever R, Kas R, Birdja YY, Diaz-Morales O, Kwon Y, Ledezma-Yanez I, Schouten KJP, Mul G, Koper MTM (2015) Electrocatalytic reduction of carbon dioxide to carbon monoxide and methane at an immobilized cobalt protoporphyrin. Nat Commun 6:8177

Sun Q, Dai Y, Ma Y, Li X, Wei W, Huang B (2015) Two-dimensional metalloporphyrin monolayers with intriguing electronic and spintronic properties. J Mater Chem C 3:6901–6907

Varela AS, Ju W, Bagger A, Franco P, Rossmeisl J, Strasser P (2019) Electrochemical reduction of CO2 on metal-nitrogen-doped carbon catalysts. ACS Catal 9:7270–7284

Wang M, Torbensen K, Salvatore D, Ren S, Joulié D, Dumoulin F, Mendoza D, Lassalle-Kaiser B, Işci U, Berlinguette CP, Robert M (2019a) CO2 electrochemical catalytic reduction with a highly active cobalt phthalocyanine. Nat Commun 10:3602

Wang X, Vasileff A, Jiao Y, Zheng Y, Qiao S-Z (2019b) Electronic and structural engineering of carbon-based metal-free electrocatalysts for water splitting. Adv Mater 31:1803625

Wang Y, Yuan H, Li Y, Chen Z (2015) Two-dimensional iron-phthalocyanine (Fe-Pc) monolayer as a promising single-atom-catalyst for oxygen reduction reaction: a computational study. Nanoscale 7: 11633–11641

Wang Z, Zhao J, Wang J, Cabrera CR, Chen Z (2018) A Co–N4 moiety embedded into graphene as an efficient single-atom-catalyst for NO electrochemical reduction: a computational study. J Mater Chem A 6:7547–7556

Yang X-F, Wang A, Qiao B, Li J, Liu J, Zhang T (2013) Single-atom catalysts: a new frontier in heterogeneous catalysis. Acc Chem Res 46:1740–1748

Yin YB, Guo S, Heck KN, Clark CA, Coonrod CL, Wong MS (2018) Treating water by degrading oxyanions using metallic nanostructures. ACS Sustain Chem Eng 6:11160–11175

Yuen AP, Jovanovic SM, Hor A-M, Klenkler RA, Devenyi GA, Loutfy RO, Preston JS (2012) Photovoltaic properties of M-phthalocyanine/fullerene organic solar cells. Sol Energy 86:1683–1688

Zhang X, Chen A, Zhang Z, Jiao M, Zhou Z (2018) Transition metal anchored C2N monolayers as efficient bifunctional electrocatalysts for hydrogen and oxygen evolution reactions. J Mater Chem A 6: 11446–11452

Zhou J, Sun Q (2011) Magnetism of phthalocyanine-based organometallic single porous sheet. J Am Chem Soc 133:15113–15119

Zhu G, Kan M, Sun Q, Jena P (2014) Anisotropic Mo2–phthalocyanine sheet: a new member of the organometallic family. J Phys Chem A 118:304–307